

1 **Probabilistic Safety Analysis using Traffic Microscopic Simulation**

2

3

4 *Carlos **Lima Azevedo**

5 Singapore MIT Alliance for Research and Technology

6 1 Create way, 138602 Singapore

7 Phone:+65 66011634

8 Fax: +65 6684 2118

9 email: cami@smart.mit.edu

10

11 João Lourenço **Cardoso**

12 National Laboratory for Civil Engineering

13 101 Av. Do Brasil, 1700-066 Lisbon, Portugal

14 Phone: +351 218443661

15 Fax: +351 218443029

16 email: jpcardoso@lnec.pt

17

18 Moshe E. **Ben-Akiva**

19 Massachusetts Institute of Technology

20 Cambridge, Massachusetts 02139, United States of America

21 Phone: +16172535324

22 Fax: +16172531130

23 email: mba@mit.edu

24

25

26 * Corresponding Author

27

28

29 Word count: 6535 + 3 Figures + 2 Tables (1250) = 7785 words

30 Submitted the 1st August 2014

31 ABSTRACT

32

33 Traffic microscopic simulation applications are currently a common tool in road system analysis
34 and several application attempts to safety performance assessment have been recently carried out.
35 However, current approaches still ignore causal relationships between different levels of vehicle
36 interactions or/and accident types, lacking a physical representation of the accident phenomena itself. In
37 this paper, a new generic probabilistic safety assessment framework for traffic microscopic simulation
38 tools is proposed. The probability of a specific accident occurrence is assumed to be estimable by an
39 accident propensity function, consisting in a deterministic safety score component and a random
40 component. The formulation of the safety score component may be specified as dependent on the type of
41 occurrence, detailed vehicle interactions and maneuvers, and on selected key simulation modelling
42 features. This generic model was applied to the case of urban motorways and specified to four types of
43 events: non-accident events and three types of accidents in a nested logit structure: rear-end and lane-
44 changing conflicts, and run-off-road events.

45 As there is still no available large disaggregated data set linking trajectories to accident
46 occurrence, artificial trajectories from a detailed calibrated microscopic simulation tool were used. These
47 trajectories were obtained following a comprehensive calibration effort: extracting trajectories for a
48 generic scenario, calibration of the simulation tool using the collected trajectories, and re-calibration of
49 the simulation model using aggregate data for each event selected for replication and used in the safety
50 model estimation phase.

51 The final estimated safety model allowed for the identification and interpretation of several
52 simulated vehicle interactions at stake. The fact that these considerations were extracted from simulated
53 analysis shows the real potential of well (detailed) calibrated traffic microscopic simulation for detailed
54 safety assessments and their potential as a lay-out design tool.

55

56

57

58 KEYWORDS

59

60 Traffic microscopic simulation; road safety; probabilistic modeling; driving behavior modeling;
61 surrogate safety measures; calibration.

62

63 1 INTRODUCTION

64 Traffic microscopic simulation applications are currently becoming a common tool in both the
65 transportation practitioners and researchers communities. The original purpose for developing such tools
66 was network efficiency assessment. The need for simultaneously assessing safety impacts of
67 transportation systems soon arose. However, despite several enhancements at the driving behaviour
68 modelling level (for a detailed review see (1)), dedicated safety modelling in simulation has been
69 frequently neglected due to the existing limited applied model formulations on driver's perception,
70 decision and error mechanisms and to the lack of data for its development.

71 With the development of many infrastructure-based Intelligent Transportation Systems, research
72 efforts have been dedicated to identify, traffic scenarios that might be used as accident precursors. Models
73 developed with this aim are referred as (real-time) accident probability models and, typically, make use of
74 aggregated real-time traffic data collected by sensing technologies (generally from loop detectors), road
75 geometric characteristics and, in some cases, weather conditions to statistically predict changes in the
76 accident occurrence probability. Some researchers opted for the use of these accident probability models
77 to perform the safety assessment in microscopic simulation experiments (2), (3) and (4). These modelling
78 streams rely on the availability of historical accident records and depend on some level of aggregation
79 regarding the traffic operations data used as explanatory variables. As accidents are considered rare events
80 and it is hard to isolate the effect of many factors affecting its occurrence, conflicts have also been used as
81 an alternative estimator of system safety (5). The use of conflicts is based on the assumption that the
82 expected number of accidents occurring on a system is proportional to the number of conflicts making
83 suitable for systems' comparisons (6). One of the main limitations of using conflicts is the correct
84 estimation of this proportionality. This difficulty has motivated the research community to develop
85 several models to estimate accident frequency from traffic conflicts counts (7). Another difficulty in using
86 conflicts for modelling purposes is the lack of practical definitions and measurement standards (as it does
87 not estimate the probability of an accident itself). For this purpose several time-based, deceleration-based
88 and dynamic-based surrogate safety performance indicators were proposed in the literature (8). Despite
89 this, these models are the most widely used within microscopic simulation studies ((9), (10), (11), (12),
90 (13)).

91 Very recently, efforts have been made to integrate interaction in probabilistic modelling
92 frameworks. While the above mentioned accident probability models try to link the probability of a
93 specific accident occurrence using a statistical model fitted to aggregated data, probabilistic frameworks
94 try to formally represent cause-effect relationships between performed driving tasks and traffic scenarios
95 that may lead to typical accident events. Such approach has a higher potential in replicating the intrinsic
96 nature of an accident mechanism and, ultimately, would not depend on safety records itself. On the other
97 hand, probabilistic frameworks depend on much more detailed information as the distributions and
98 relationships between all variables at stake are needed (e.g.: evasive manoeuvres probabilities for
99 different situations or pavement conditions for different scenarios). Songchitruksa and Tarko (14)
100 proposed an Extreme Value (EV) approach to build up relationships between occurrence of right-angle
101 accidents at urban intersections and frequency of traffic conflicts measured by using PET as accident
102 proximity variable. Saunier and Sayed (15) developed a comprehensive probabilistic framework for
103 automated road safety analysis based on motion prediction. Wang et al. (16) propose an incident tree
104 model and an incident tree analysis method for the identification of potential characteristics of accident
105 occurrence in a quantified risk assessment framework. These efforts step forward in a more
106 comprehensive formulation of the accident phenomena, but still haven't been widely validated or
107 integrated in simulation tools for practical application. Several simulation-based safety studies were also
108 documented in a very recent and comprehensive review by Young et al. (17). In summary, the authors
109 clearly pointed out the need for analysing the probabilistic nature of the link between the vehicle
110 interaction and the accident itself and for generalising the models to accommodate for different types of
111 accidents. Furthermore, the need was recognized for differentiating distinct cause-effect relationships for
112 diverse types of accidents and for a probabilistic formulation without the limitations resulting from the

113 aggregation of both traffic data and safety records.
114

115 2 GENERIC MODEL FORMULATION

116 A generic framework for modelling cause-effect mechanisms between detailed vehicle
117 interactions from simulated environments and the accident occurrence probability is proposed. It is first
118 assumed that the state of a vehicle n at any given time t can be viewed as a discrete variable whose state
119 outcome k can be one of different types of accident or no accident at all. An individual outcome k among
120 all possible outcomes K is considered to be predicted if its probability $P_{n,t}(k)$ is maximum. As in previous
121 research studies, the main difficulty is how to estimate $P_{n,t}(k)$. This probability should be a function of
122 specific observed variables characterizing the interaction between vehicles (14). Such considerations step
123 away from the assumption of a fixed coefficient model converting the surrogate event frequency into
124 accident frequency, typically used in the traffic conflicts technique. The probability for a specific accident
125 involving vehicle n to occur at time t is assumed to be estimable by a specific accident propensity (or
126 proximity) measure (18):

$$P_{n,t}(k) \sim U_k \quad (1)$$

127 In the proposed model, each accident propensity function U_k , is considered to have a
128 (deterministic) safety score (V_k) component and a random component (ε):

$$U_k = V_k(X, \beta) + \varepsilon \quad (2)$$

129 where X is the vector of explanatory variables, β is the vector of unknown parameters to be estimated and
130 ε is the random term (the terms n and t were omitted for simplicity). The assumption of the deterministic
131 safety score component agrees with the recent research stream where detailed interaction variables
132 directly affect the accident occurrence probability itself. The random component ε is assumed to represent
133 the unobserved effects involved in the determination of the outcome; these may be derived from a random
134 process in the occurrence of a specific event or caused by a lack of knowledge of this process.

135 As it is common in safety modeling research, the accident phenomenon relies on many different
136 variables:

$$V_k(n, t) = f_k(X_{n,t}, X_{n',t}, X_{D,t}, X_S) \quad (3)$$

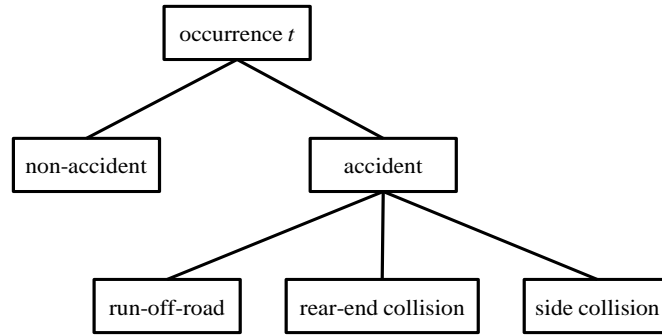
137 where the k accident-type specific scoring function f_k depends on: $X_{n,t}$, the driver-vehicle unit n specific
138 variables at time t ; $X_{n',t}$, the variables at time t for the interaction between n and a conflicting driver-
139 vehicle unit n' ; $X_{D,t}$, the dynamic environmental variables at time t (e.g.: weather, variable speed limit,
140 lighting conditions, etc); and X_S , the static environmental variables (e.g.: geometrics, road signs, etc).
141 Note that driver characteristics are typically not considered in traffic simulation tools, which substantially
142 limits the number of available candidate explanatory variables $X_{n,t}$.

143 In the presented model we framed the formulation of each function f_k to represent a cause-effect
144 relationship, to simultaneously deal with different non-independent types of accident outcomes and to
145 consider a disaggregated probability for any vehicle state (n, t) observation (instead of the existing
146 aggregate formulation used in real-time accident probability models).
147

148 3 MODELLING DIFFERENT ACCIDENT TYPES

149 The above general formulation is now detailed to a specific set of accidents that typically occur
150 on busy urban motorways: rear-end accidents, side collisions during lane-change maneuvers and run-of-
151 road accidents. It is clear that these three different outcomes correspond to very distinct phenomena.

152 However, it is also known that these three outcomes may be related, namely if one considers accident
 153 outcomes following an evasive action from different risky interactions (see FIGURE 1):



154

FIGURE 1 Model structure for motorway accident occurrence

155

156 3.1 Rear-end (RE) conflicts

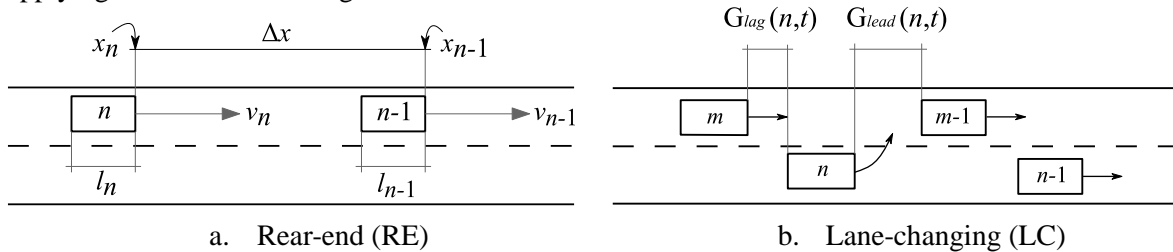
157 When facing rear-end interactions the probability of a collision is formulated in terms of: the
 158 subject vehicle braking requirements to avoid a RE collision and the maximum available braking power.
 159 The first is represented by the difference between the actual relative acceleration between the subject
 160 vehicle n and its leader $(n - 1)$, Δa (m/s^2), and the deceleration rate required to avoid crash, DRAC (m/s^2),
 161 estimated using Newtonian physics:

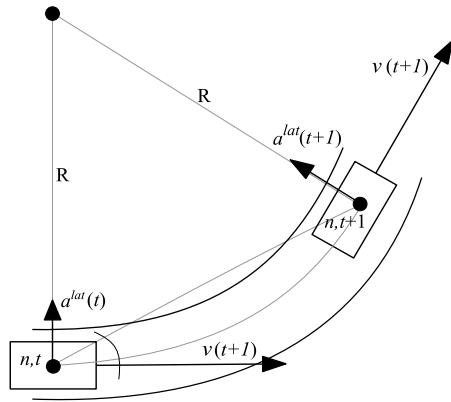
$$\Delta a^{\text{need}}(n, t) = \text{DRAC}(n, t) + \Delta a(n, t) \quad (4)$$

$$\text{DRAC}(n, t) = \frac{[v(n - 1, t) - v(n, t)]^2}{2[x(n - 1, t) - x(n, t) - l(n)]} \quad (5)$$

162 where $v(n, t)$, $x(n, t)$ and $l(n)$ are the speed, longitudinal position and length of vehicle n (FIGURE 2.a).

163 We further split of the needed deceleration rate into its positive, $\Delta a_+^{\text{need}}(n, t) \geq 0$, and negative,
 164 $\Delta a_-^{\text{need}}(n, t) \leq 0$, components, allowing for the consideration of different parameters. The advantage of
 165 using Δa^{need} instead of just the DRAC is the consideration of the current acceleration state. The value of
 166 Δa^{need} is easily interpreted: the negative values represent safer values, for which the vehicle is already
 167 applying a deceleration rate greater than DRAC.





c. Run-off-road (ROR)

FIGURE 2 Accident outcomes

168 We further improve this formulation by dividing the required deceleration by the time-to-
 169 collision, TTC, thus considering also how long the driver has before the potential collision. The RE safety
 170 score function will then depend on the available time for adjustment, resulting in a relative needed
 171 deceleration ratio $RA^{\text{need}}(n, t)$:

$$RA^{\text{need}}(n, t) = \frac{\Delta a^{\text{need}}(n, t)}{TTC(n, t)} \quad (6)$$

$$TTC(n, t) = \frac{x(n-1, t) - x(n, t) - l(n)}{(v(n, t) - v(n-1, t))} \quad (7)$$

172 Finally, similarly to the CPI surrogate safety measure described in (6), a measure of the maximum
 173 available deceleration rate is also considered. It allows considering heterogeneous safety conditions
 174 regarding different vehicle categories and different pavement conditions (e.g.: dry/wet) that are expected
 175 to influence the deceleration performance:

$$\Delta a^{\text{lim}}(n, t) = DRAC(n, t) - (\mu^{\text{long}}(n, t) + d)g \quad (8)$$

$$\mu^{\text{long}}(n, t) = f^{\text{long}}(v(n, t), \alpha^{\text{type}}, \alpha^{\text{wet}}) \quad (9)$$

176 where $\Delta a^{\text{lim}}(n, t)$ is the maximum available deceleration for vehicle n at time t , d is the grade rate (m/m),
 177 g is the gravitational acceleration of 9.81 m/s^2 and $\mu^{\text{long}}(n, t)$ is the maximum available longitudinal
 178 friction coefficient, which depends on the speed of the vehicle itself $v(n, t)$ and on two factors that
 179 account for the vehicle type, α^{type} , and the pavement condition, α^{wet} . This simplified formulation of the
 180 friction coefficient is due to the small number of variables typically available in simulated environments.
 181 Similarly to the previous variables, the rate $RA^{\text{lim}}(n, t) = \Delta a^{\text{lim}}(n, t)/TTC(n, t)$ is used in the safety
 182 score function to account for the TTC.

183 The systematic safety score for RE collisions may now be formulated as:

$$V_{\text{RE}}(n, t) = \beta_0^{\text{RE}} + \beta_1^{\text{RE}} RA_+^{\text{need}}(n, t) + \beta_2^{\text{RE}} RA_-^{\text{need}}(n, t) + \beta_3^{\text{RE}} RA^{\text{lim}}(n, t) \quad (10)$$

184 where RA_+^{need} and RA_-^{need} are the positive and negative components of the relative needed deceleration

185 ratio computed using Δa_+^{need} and Δa_-^{need} respectively; RA^{lim} is the maximum available deceleration ratio;
 186 and β_0^{RE} , β_1^{RE} , β_2^{RE} and β_3^{RE} are the estimable parameters.
 187

188 3.2 Lane-changing (LC) conflicts

189 The lane change action decision is typically modelled by means of gap acceptance models (19)
 190 or, alternatively, by acceleration variation models (20). One would expect the probability of lane-change
 191 collisions to be function of vehicles lateral movements. However, the large majority of the current micro-
 192 simulation tools do not provide this modelling feature. Therefore, surrogate measures depending on
 193 lateral movements, such as the time-to-lane-crossing proposed in (21) and the Post-Encroachment-Time
 194 used in (22), are not easily integrated.

195 The probability of a LC collision is based on gap acceptance models and formulated in terms of
 196 gap variation. The gap acceptance is generally modelled separately regarding the lead and the lag gaps on
 197 the target lane (FIGURE 2.b**Error! Reference source not found.**). This disaggregation is of special
 198 interest as different parameters may be computed for different gaps (23). It is known that the lane-
 199 changing process becomes increasingly difficult as the speed differences between the subject vehicle and
 200 the lead and lag vehicles in the target lane increases (24). Thus, in the proposed formulation, the safety
 201 score of the LC event is specified in terms of relative gap variation:

$$RG^{\text{gap}}(n, t) = \frac{\Delta v^{\text{gap}}(n, t)}{G^{\text{gap}}(n, t)} \quad (11)$$

202 where G^{gap} is the gap in meters and Δv^{gap} represents the speed difference between the subject vehicle
 203 and the lead (or lag) vehicle on the target lane in m/s:

$$\Delta v^{\text{lead}}(n, t) = v(m - 1, t) - v(n, t) \quad (12)$$

$$\Delta v^{\text{lag}}(n, t) = v(n, t) - v(m, t) \quad (13)$$

204 Where $v(m - 1, t)$ and $v(m, t)$ are the speed of the lead vehicle $m - 1$ and the lag vehicle m in
 205 the target lane, respectively. Again, the split of the relative gap variation into its positive, RG_+^{gap} , and
 206 negative, RG_-^{gap} values allows for the consideration of different parameters associated with different
 207 safety conditions, i.e. for gaps that are either increasing or decreasing, respectively.

$$RG_+^{\text{gap}}(n, t) = \max(0, RG^{\text{gap}}(n, t)) \rightarrow RG_+^{\text{gap}}(n, t) \geq 0 \quad (14)$$

$$RG_-^{\text{gap}}(n, t) = \min(0, RG^{\text{gap}}(n, t)) \rightarrow RG_-^{\text{gap}}(n, t) \leq 0 \quad (15)$$

208 Following the above formulation a gap with a higher relative shrinking rate ($RG_-^{\text{gap}}(n_1, t_1) <$
 209 $RG_-^{\text{gap}}(n_2, t_2) \leq 0$), for example, should have a higher impact on the LC conflict probability,
 210 $P_{n_1, t_1}(\text{LC}) > P_{n_2, t_2}(\text{LC})$, and therefore, its parameter estimate should be negative.
 211

The systematic component for LC collisions may now be formulated as:

$$V_{\text{LC}}(n, t) = \beta_0^{\text{LC}} + \beta_1^{\text{LC}} RG_+^{\text{lag}}(n, t) + \beta_2^{\text{LC}} RG_-^{\text{lag}}(n, t) + \beta_3^{\text{LC}} RG_+^{\text{lead}}(n, t) + \beta_4^{\text{LC}} RG_-^{\text{lead}}(n, t) \quad (16)$$

212 where RA_+^{gap} and RA_-^{gap} are the positive and negative components (with $\text{gap} = \{\text{lead}, \text{lag}\}$) and β_0^{LC} , β_1^{LC} ,
 213 β_2^{LC} , β_3^{LC} and β_4^{LC} are the estimable parameters.
 214

215 3.3 Run-off-road (ROR) events

216 ROR events are assumed as being primarily related to individual vehicle dynamics rather than
 217 interaction with others. This assumption is especially true under free-flow scenarios. However, it may also
 218 result from evasive manoeuvres due to risky lane-changing or car-following decisions.

219 Vehicle dynamics in traffic simulation models are represented in a much simplified manner when
 220 compared with the detailed movements' description of real events and its representation currently
 221 achieved with accident reconstruction models. This significantly limits the current potential for a ROR
 222 micro-simulation modelling framework. The vehicle lateral movement, the true road geometric
 223 characteristics (such as transition curves), the pavement surface characteristics, and the vehicle detailed
 224 physical and mechanical attributes are generally not available. However, some relevant variables that may
 225 potentially be useful for the analysis of ROR events are already available in micro-simulation tools, such
 226 as vehicle speed, general road geometrics and the generic vehicle type.

227 In the proposed framework, the safety score of ROR events is assumed to be linked to the
 228 difference between the current lateral acceleration of vehicle n and a site specific critical lateral
 229 acceleration. First, as vehicle lateral movements and the true road geometrics are not modelled, the
 230 vehicle path on curve elements is assumed as a simple circular path and the vehicle yaw equal to the
 231 curve bearing (FIGURE 2.c). The lateral acceleration of vehicle n , a_{lat} , is therefore derived from its
 232 current speed and the curve radius R (m):

$$a^{lat}(n, t) = \frac{[v(n, t)]^2}{R} \quad (17)$$

233 Although the majority of the simulation tools do not provide information on lateral movement
 234 during a lane change, it is expected that this type of manoeuvres will also affect the ROR event
 235 probability. Using test track data, Chovan et al. (23) considered peak lateral acceleration values of 0.4g,
 236 0.55g and 0.7g for mild, moderate, and aggressive steering manoeuvres, respectively. As detailed lane
 237 change models are typically not available in microscopic traffic simulation platforms, a generic peak
 238 acceleration add-on for lane change of 0.5g was adopted and integrated in eq. 17 to account for a potential
 239 increased ROR probability in road sections with high frequency of lane:

$$a^{lat}(n, t) = \frac{[v(n, t)]^2}{R} + 0.5g\delta^{lc}(n, t) \quad (18)$$

240 where $\delta^{lc}(n, t)$ is a dummy variable to account for lane change (1 if the vehicle is performing a lane
 241 change, 0 otherwise).

242 The maximum allowed lateral acceleration $a_{cr}^{lat}(n, t)$ directly depends on the critical lateral
 243 friction coefficient μ^{lat} and the road super-elevation e (m/m):

$$a_{cr}^{lat}(n, t) = (\mu^{lat}(n, t) + e)g \quad (19)$$

244 Similarly to its longitudinal counterpart, the values of the maximum lateral friction coefficient,
 245 μ^{lat} , also depend on the vehicle speed itself v , on the pavement condition (wet/dry) and on the type of
 246 vehicle:

$$\mu^{lat}(n, t) = f^{lat}(v(n, t), \alpha^{type}, \alpha^{wet}) \quad (20)$$

247 The safety score function may now be formulated in terms of the positive (unsafe) and negative
 248 (safe) components of the difference between the current and the critical lateral accelerations:

$$V_{\text{ROR}}(n, t) = \beta_0^{\text{ROR}} + \beta_1^{\text{ROR}} \Delta a_+^{\text{lat}}(n, t) + \beta_2^{\text{ROR}} \Delta a_-^{\text{lat}}(n, t) \quad (21)$$

249 where Δa_+^{lat} and Δa_-^{lat} are the positive and negative components of $\Delta a^{\text{lat}} = a^{\text{lat}} - a_{\text{cr}}^{\text{lat}}$, respectively.
250

251 3.4 Estimation framework

252 As previously stated, the explanatory variables of one type of accident may influence the
253 occurrence of others and evasive manoeuvres may create correlations between different accident
254 outcomes. When modelling multiple discrete outcomes, the multinomial nested logit model proposed by
255 Ben-Akiva (25) has advantages over the simple multinomial logit model, because it can simultaneously
256 estimate the influence of independent variables while allowing for the error terms to be correlated and,
257 therefore, allowing for the violation of the independence of irrelevant alternatives (IIA) property (the
258 reader is referred to (26), for its derivation and formulation details).

259 To directly estimate the proposed model, a large set of all types of model outcomes and its vehicle
260 interaction data is needed. Unfortunately, a large data allowing for the direct association between
261 trajectories and accident occurrence is still not available. Furthermore, although the proposed model is
262 specified individually for any vehicle n at every time t , the philosophy of microscopic simulation
263 applications is to replicate as close as possible real aggregate measurements, even at such detailed level as
264 aggregated accelerations, headways or TTC. Thus, to estimate the above model the use of artificial
265 (simulated) trajectories is proposed. Yet, a set of critical assumptions must be considered:

- 266 1. A well calibrated microscopic simulation model must be calibrated appropriately to replicate
267 statistical distributions of detailed traffic variables..
- 268 2. Trajectories extracted in a generic day represent the general driving behaviour of traffic.
269 Confidence on this assumption depends on the amount and breath of information available for
270 treatment. Other factors (such as weather) influence general driving behaviour parameters;
271 part of this variability will be assessed by means of a dedicated calibration, carried out for
272 each specific event, using readily available data sets (eg.: from loop sensors).
- 273 3. Although simulation models are accident free, their description of detailed traffic variables
274 can be linked to the accident probability. This is supported by previous studies (9), (2).

275 The microscopic simulation tool is then calibrated once using the pre-estimated seed Origin-
276 Destination (OD) matrix, and both aggregate (loop sensor based) and disaggregate (observed vehicle
277 trajectories) data collected for a specific generic day d_0 . The optimum sets of the microscopic simulation
278 model parameters β_0 are then used as initial parameters in an aggregate calibration process using the
279 aggregated data available for each event observation i . After this, the optimum set of parameters for each
280 event i , β_i , is used to generate a set of (artificial) detailed traffic variables. Finally, this set of detailed
281 traffic variables is used jointly with its associated outcome of event i to estimate the proposed safety
282 model.

283 It is typically expected that both the loop-based variables used for calibration and the accident
284 occurrence reported variables are defined for a pre-defined time and spatial units. In some cases, such
285 aggregated intervals maybe too large to capture short-term variations; nevertheless several authors (27),
286 (2) have successfully used aggregated periods up to 5 min intervals to perform accident occurrence
287 probability analyses. With the absence of true trajectory variables for the vehicle n involved in each
288 observed event i , the characterization of the detailed traffic variables for a specific accident occurrence
289 must be linked by means of spatial and temporal aggregation. Additionally, it is well known that safety
290 records have time and spatial errors. Therefore, for estimation one needs to aggregate all vehicle state
291 outcome probabilities $P_{n,t}(k)$ by standardized intervals of space, s , and time periods, p :

$$P_{s,p}(k) = \frac{1}{N} \sum_N P_{n,t}(k) \quad (22)$$

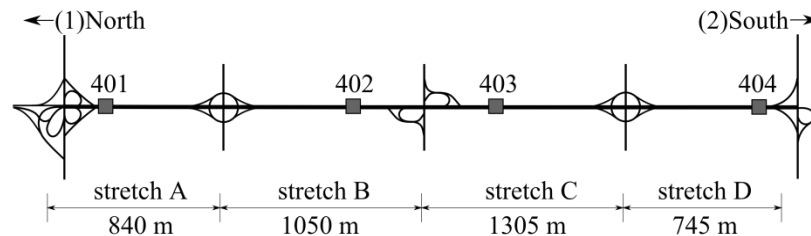
292 where $P_{n,t}(k)$ is the probability of occurrence k for any relevant observation of vehicle n at time t ,
 293 traveling in spatial interval s and time period p and defined by the proposed nested logit model; N is the
 294 total number of observations for all vehicles that travelled in the interval s, p . It is important to point out
 295 that, following this formulation, the model is based on mean values and not on extreme values. This
 296 follows the traffic micro-simulation specification philosophy, where the replication of averaged variables
 297 is expected. However, one may want to push the use of extreme formulations and rely on detailed
 298 calibration methods of extreme values, or by extending the specification of the driver behaviour to better
 299 model such scenarios. Such formulation was not tested for the present document.

300 Finally, if one considers a large observation period, typically needed to have a relevant number of
 301 accident occurrences, it is expected that the loop sensors will fail for some instances. Furthermore, the
 302 computational memory and processing resources needed to generate and use the simulated trajectory data
 303 for a large set of no-accident occurrence units is impractical. For this purpose an outcome (choice)-based
 304 random sampling was assumed. Then, to account for this biased sampling process the weighted
 305 exogenous sample maximum likelihood function (WESML) proposed in (29) was used.

306

307 4 THE URBAN MOTORWAY CASE AND TESTING DATASET

308 The proposed model was estimated using collected and simulated data for the A44 urban
 309 motorway near Porto, Portugal. This road was selected as case study due to its dense traffic, unusually
 310 high number of lane changes, short spacing between interchanges and high percentage of heavy goods
 311 vehicles. A44 is a 3,940m long dual carriageway urban motorway with 5 major interchanges, two 3.50m
 312 wide lanes and 2.00m wide shoulders in each direction (FIGURE 3). There are acceleration and
 313 deceleration lanes at all interchanges, although several as short as 150m. On and off-ramps connect to
 314 local roads, which generally have tight horizontal curves, intersections or pedestrian crossings, features
 315 that tend to impose significant reductions in vehicle speeds.



316

FIGURE 3 A44 Layout

317 Three different traffic data sets were specifically collected for the present study: a dynamic seed
 318 OD based on a sample of license plate matching and vehicle counts (Lima Azevedo, 2014); 5 min loop
 319 sensor average speeds and counts for the existing eight traffic stations (4 in each direction), between 2007
 320 and 2009 (30); and vehicle trajectories collected for a generic morning (with and without congestion) by
 321 aerial remote sensing for the entire length and access links of the A44 motorway (31). Finally, incident
 322 records were also collected for the same period of 2007 to 2009 including a total of 144 side-collisions
 323 rear-end collisions and run-off-road accidents.

324 Along with the 5 min temporal units for the observed traffic data, the nature of the accident
 325 location record required a spatial observation unit of 50 m. These units are the ones to be considered for
 326 the aggregation of individual probabilities. Using such units, a very large number of no-accident (NA)
 327 events were observed during this three years period (more than 180×10^6). After excluding the days with
 328 bad sensor data, a random sampling technique was used to select 6,400 no-accident events, resulting in a
 329 total of 6,544 events to be calibrated and simulated for artificial data generation.

330 The integrated driver behaviour model (19) implemented in MITSIMLab (32) was used to
 331 simulate trajectories for each observed event. For the calibration, the global multi-step sensitivity-analysis
 332 based calibration proposed in (33) was used. The method was then coupled with a meta-model based

333 calibration for calibrating the simulator with trajectory data and with a powerful simultaneous demand-
 334 supply calibration method for the calibration of the large set of accident and non-accident events using
 335 aggregated data (34). This procedure was selected, as it was concluded in previous work (34) that
 336 disaggregate calibration improves significantly the accuracy of simulated trajectories and spot-speeds,
 337 which are important for adequate representation of vehicle interactions in safety studies.

338 The artificial data generated by the calibrated models showed a clear divergence between accident
 339 and non-accident event simulated outputs typically used in safety assessment (see detailed statistics in
 340 (30)).

341 5 ESTIMATION RESULTS

342 5.1 Modeling assumptions

343 For the computation of the RE and ROR model components, both μ_{long} and μ_{lat} must be
 344 specified. Unfortunately, on-site measured values were not available. Hence, generic μ_0 values were
 345 adopted based on measurements from other urban freeways found in the literature (Inoue and Hioki,
 346 1993): a direct variation from 0.85 at 0km/h to 0.75 at 130km/h for dry pavements and from 0.70 at
 347 0km/h to 0.20 at 130km/h for wet pavements. An increase factor of 1.10 was considered for the lateral
 348 coefficient μ_{lat} . Furthermore, both μ_{long} and μ_{lat} were decreased by a factor of 0.70 for heavy vehicles in
 349 dry conditions.

350 The availability of each occurrence alternative was included in the specification of the likelihood
 351 function. For each observation:

- 352 • a rear-end conflict was considered as possible whenever the subject vehicle is in a car-following
 353 state;
- 354 • a lane change conflict was considered as possible if the road carriageway has two or more lanes
 355 and if the subject vehicle wants to perform a lane change;
- 356 • a run-of-road event was considered as possible if the road section is a curve or if the subject
 357 vehicle is performing a lane-change.

358 Finally, multiple replications should be used directly in the estimation phase within a Monte
 359 Carlo process, similar to panel data estimation. With this approach, several observations for the same
 360 event are available and directly included in the safety score function with an additional event specific
 361 component. The main burden in such an approach is the computer memory and processing resources
 362 needed during the estimation phase. In the current study, the estimation process was carried out
 363 considering each replication as independent.

364 The maximum likelihood estimates of the model parameters are calculated by maximizing this
 365 function:

$$\mathcal{L} = \sum_{s,p} \sum_k y_{k,s,p} w_k \ln[P_{s,p}(k)] \quad (23)$$

366 where k are all possible outcomes considered for the proposed model $P_{s,p}(k)$ is the probability of outcome
 367 k for spatial interval s and time period p (given by equation 22), w_k is the outcome k -specific sampling
 368 ratio, $y_{k,s,p}$ is 1 if k is the observed outcome for the observation pair s, p and 0 otherwise. In this study,
 369 the PythonBIOGEME open source software was used (36).

370 Finally, for numerical reasons, it is good practice to scale the data so that the absolute values of
 371 the parameters are between zero and 1; thus, all relative gap variation variables were divided by 10 and
 372 the lateral acceleration difference specified in 0.1m/s^2 .

373

374 5.2 Results

375 The estimation results are presented in TABLE 1.

376 When the positive RA^{need} component is close to zero, the relative deceleration is close to the
 377 DRAC and thus closer to a safe situation. When RA_+^{need} increases the probability for a RE accident is
 378 higher, as the difference between the vehicle relative deceleration rate and its DRAC gets higher. β_1^{RE} has
 379 a higher absolute magnitude than β_2^{RE} , penalizing much more any safety decay in the unsafe domain
 380 ($RA^{need} > 0$) rather than in the safe one ($RA^{need} < 0$). Regarding the negative component, i.e. when the
 381 follower has already adjusted its acceleration, lower RA_-^{need} will result in an increased RE probability due
 382 to lower TTC. The positive sign of β_3^{RE} and its statistical significance makes the consideration of different
 383 exogenous safety conditions non-negligible. It is worth pointing out that both the vehicle category
 384 (car/truck or bus) and the pavement (wet/dry) conditions were considered.

385 The parameters of the negative components of the lead and lag gaps variation during LC events
 386 (β_2^{LC} and β_4^{LC}) are also significant: largest absolute values of its independent variables (RG_-^{lag} and RG_-^{lead})
 387 represent significantly shrinking gaps. As both parameters are negative, any RG_-^{lag} or RG_-^{lead} will increase
 388 the probability of LC accident events. The lead relative gap variation came out as the most statistically
 389 significant regarding LC events and its higher magnitude is due to the much smaller simulated lead gaps
 390 during lane-change not only when compared to lag gaps but also when comparing accident events with
 391 no-accidents.
 392

TABLE 1 Estimation results.

| Event | Parameter | value | st. dev. | t-stat | p-val |
|-----------------------------|---|---------|----------|--------|-------|
| | RE constant β_0^{RE} | -13.09* | 0.608 | -5.08 | <0.01 |
| Rear-end conflict | Positive relative needed dec. β_1^{RE} | 2.917 | 0.917 | 3.18 | 0.01 |
| | Negative relative needed dec. β_2^{RE} | -1.92 | 0.784 | -2.45 | 0.03 |
| | Maximum available dec. ratio β_3^{RE} | 2.03 | 1.034 | 1.96 | 0.07 |
| | LC constant β_0^{LC} | -7.08* | 0.457 | 6.32 | <0.01 |
| Lane- change conflict | Positive relative lag gap variation β_1^{LC} | -0.011 | 0.012 | -0.92 | 0.38 |
| | Negative relative lag gap variation β_2^{LC} | -0.568 | 0.338 | -1.68 | 0.12 |
| | Positive relative lead gap variation β_3^{LC} | -0.311 | 0.255 | -1.22 | 0.25 |
| | Negative relative lead gap variation β_4^{LC} | -0.628 | 0.315 | -1.99 | 0.07 |
| | ROR constant β_0^{ROR} | -12.45* | 0.367 | -6.68 | <0.01 |
| Run-off- road event | Positive lateral acc. difference β_1^{ROR} | 0.023 | 0.013 | 1.77 | 0.10 |
| | Negative lateral acc. difference β_2^{ROR} | 1.775 | 0.965 | 1.84 | 0.09 |
| | Scale parameter for the accident nest μ | 1.622 | 0.567 | 2.86 | 0.01 |

N° of parameters 13 (* are the parameters affected by weights)

Sample size: 10733084 (3 replications)

Initial log-likelihood: -9636.49

Final log-likelihood: -2047.53

ρ^2 : 0.787

$\bar{\rho}^2$: 0.786

393 Regarding ROR events, when Δa^{lat} is positive, the simulated lateral acceleration is higher than
 394 the critical lateral acceleration and the vehicle is under unsafe conditions. Thus, when $\beta_1^{ROR} > 0$ there is a
 395 higher probability of ROR events. Similarly, when Δa^{lat} is negative, larger absolute values are related to
 396 safer conditions, as the simulated lateral acceleration is much smaller than the critical one ($\beta_2^{ROR} < 0$). Yet,
 397 one would expect a higher absolute magnitude for β_1^{ROR} , but these results may be justified with the small
 398

399 number of observations with $\Delta a^{\text{lat}} > 0$.

400 The estimated scale parameter of the accidents nest μ was also significant, revealing a non-
401 negligible effect of shared unobserved attributes of the different types of accident under analysis.

402

403 6 VALIDATION

404 As no other accident data set was available, the validation was performed using two new sets of
405 artificial data, generated by MITSIMLab for the same sample of events.

406 In **TABLE 2** the averaged ratios of the probabilities between a specific type of accident and the
407 no-accident events are presented for both the estimation and validation data sets. The range of both input
408 variables and estimated probabilities for the validation data set are similar to the estimation ones. The
409 trade-offs (correlations) captured by the model are also visible, especially between RE and LC conflicts.

410

TABLE 2 Validation probability ratios regarding P(NA).

| | | P(RE) | P(LC) | P(ROR) |
|------------|-----|-------|-------|--------|
| Estimation | RE | 3.783 | 3.880 | 0.359 |
| | LC | 2.284 | 3.581 | 0.468 |
| | ROR | 1.755 | 0.499 | 1.241 |
| Validation | RE | 4.352 | 5.824 | 0.344 |
| | LC | 2.363 | 3.027 | 0.391 |
| | ROR | 1.306 | 0.277 | 1.299 |

411

412 The accuracy rates for all accident events considered was 38.6% using the validation data set. The
413 accuracy for non-accident events was 92.1% while false alarms reached 7.9%. In a previous model using
414 real loop sensor data, Oh et al. (2001) estimated the prediction accuracy for accidents and non-accidents
415 as 55.8% and 72.1%, and a false alarm rate of 27.9%. Xu et al. (37) estimated the same rates as 61.0%,
416 80.0% and 20.0%, respectively. The rates obtained with the proposed model with artificial data still
417 remain below the values found in the literature for aggregated accident probability models using real data.
418 The small sample used for estimation may have affected this number. Yet, the false alarm rate is
419 considerably lower than values reported in other studies, indicating a high specificity of the proposed
420 model.

421

422 7 CONCLUSIONS

423 A generic framework for modelling cause effect mechanisms between detailed traffic variables
424 and accident occurrence probability in traffic microscopic simulation tools was proposed and tested in a
425 real road environment. Detailed variables of vehicle motion and interactions were found to be linked to
426 different accident increased probabilities. The nested structured allowed to capture existing trade-offs
427 between different types of accidents. The fact that all these considerations were extracted from simulated
428 analysis shows the real potential of advanced traffic microscopic simulation regarding detailed safety
429 assessments, as long as detailed calibration is successfully carried out. The interaction between vehicle
430 gaps and relative motions has been proved as a key factor for accident occurrence in previous safety
431 related studies. Yet, no probabilistic formulation accommodating such interaction and integrated in traffic
432 simulation models had previously been reported in the literature.

433 Several enhancements regarding the specific formulation of the proposed probabilistic safety
434 model for urban motorways may be introduced. The inclusion of further components in the safety scoring
435 function (e.g.: driver related variables), the formulation of non-linear safety score functions, the
436 specification of additional accident types and the definition of more powerful modelling structures, such

437 as the mixed logit, or estimation methods, such as a panel data estimation based on multiple replications,
438 should be tested. Also, both the validation using other sets of data and traffic scenarios and a benchmark
439 against alternative non-probabilistic safety assessment tools would be valuable. The availability of large
440 detailed trajectory data sets from naturalistic studies will be also a key source for potential improvements.
441 Furthermore, the integration of conceptual perception and error modelling frameworks and more detailed
442 motion descriptions in microscopic simulation tools may mitigate some of the modelling constraints.
443 Finally, it is worth remembering that the modelling and estimation structures were formulated in terms of
444 expected behavioural considerations but constrained by the driving behaviour simulation model
445 limitations. In fact, when a safety assessment model (probabilistic or not) is integrated into a simulation
446 tool, the safety formulation should also consider the modelling assumptions and limitations of the traffic
447 simulator itself.

448 **BIBLIOGRAPHY**

- 449 (1) Barceló, J. (ed.), 2010. *Fundamentals of Traffic Simulation*, 1st Edition. Springer.
- 450 (2) Abdel-Aty, M., Pemmanaboina, R., Hsia, L., 2006. "Assessing crash occurrence on urban freeways
451 by applying a system of interrelated equations. In: *Proceedings of the 85th Annual Meeting of the*
452 *Transportation Research Board*. Washington D.C., USA.
- 453 (3) Abdel-Aty, M., Pande, A., Lee, C., Gayah, V., 2007. "Crash risk assessment using intelligent
454 transportation systems data and real-time intervention strategies to improve safety". *Journal of*
455 *Intelligent Transportation Systems* 11 (3), 107–120.
- 456 (4) Abdel-Aty, M., Gayah, V., 2010. "Real-time crash risk reduction on freeways using coordinated and
457 uncoordinated ramp metering approaches". *ASCE Journal of Transportation Engineering* 136 (5).
- 458 (5) Hydén, C., 1987. *The development of a method for traffic safety evaluation: The Swedish Traffic*
459 *Conflicts Technique*. Technical Report, Lund University, Sweden.
- 460 (6) Cunto, F. and Saccomanno, F. F., 2008. "Calibration and validation of simulated vehicle safety
461 performance at signalized intersections". *Accident Analysis & Prevention* 40 (3), 1171-1179.
- 462 (7) Gettman, D., Sayed, T., Pu, L., Shelby, S., 2008. *Surrogate Safety Assessment Model and Validation*.
463 Technical Report. Federal Highway Administration, Virginia, USA
- 464 (8) Lareshyn, A., Svensson, A., Hydén, C., 2010. "Evaluation of traffic safety, based on microlevel
465 behavioral data: theoretical framework and first implementation". *Accident Analysis & Prevention*
466 42 (6), 1637–1646.
- 467 (9) Archer, J., 2005. *Indicators for traffic safety assessment and prediction and their application in*
468 *micro-simulation modelling : A study of urban and suburban intersections*. Ph.D. thesis, KTH -
469 Royal Institute of Technology, Sweden.
- 470 (10) Ozbay, K., Yang, H., Bartin, B., Mudigonda, S., 2008. "Derivation and Validation of a New
471 Simulation-based Surrogate Safety Measure". *Transportation Research Record: Journal of*
472 *Transportation Research Board*, 2083, 105-113.
- 473 (11) Dijkstra, A., Marchesini, P., Bijleveld, F., Kars, V., Drolenga, H., Maarseveen, M. V., 2010. "Do
474 Calculated Conflicts in Microsimulation Model Predict Number of Crashes?". *Transportation*
475 *Research Record: Journal of the Transportation Research Board* 2147, 105–112.
- 476 (12) Okamura, M., Corporation, A., Fukuda, A., Morita, H., Suzuki, H., Nakazawa, M., 2011. "Impact
477 evaluation of a driving support system on traffic flow by microscopic traffic simulation". In: *3rd*
478 *International Conference on Road Safety and Simulation*. Indianapolis, USA.

- 479 (13) Huang, F., Liu, P., Yu, H., Wang, W., Jan. 2013. Identifying if VISSIM simulation model and
480 SSAM provide reasonable estimates for field measured traffic conflicts at signalized intersections.
481 *Accident; analysis and prevention* 50, 1014–24.
- 482 (14) Songchitruksa, P., Tarko, A. P., 2006. “The extreme value theory approach to safety estimation”.
483 *Accident Analysis & Prevention*, 38 (4), 811–822.
- 484 (15) Saunier, N., Sayed, T., 2008. “Probabilistic Framework for Automated Analysis of Exposure to Road
485 Collisions”. *Transportation Research Record: Journal of the Transportation Research Board* 2083,
486 96–104.
- 487 (16) Wang, W., Jiang, X., Xia, S., Cao, Q., 2010. Incident tree model and incident tree analysis method
488 for quantified risk assessment: An in-depth accident study in traffic operation. *Safety Science* 48
489 (10), 1248–1262.
- 490 (17) Young, W., Sobhani, A., Lenné, M. G., Sarvi, M., 2014. “Simulation of safety: A review of the state
491 of the art in road safety simulation modelling”. *Accident Analysis & Prevention*, 66 (C), 89–103.
- 492 (18) Tarko, A. P., Davis, G., Saunier, N., Sayed, T., Washington, S. P., 2009. *Surrogate Measures of*
493 *Safety: A White Paper*. Technical Report n.3, Transportation Research Board. ANB20 - Committee
494 on Safety Data Evaluation and Analysis, USA.
- 495 (19) Toledo, T., Koutsopoulos, H., Ben-Akiva, M. E., 2007. “Integrated driving behavior modeling”.
496 *Transportation Research Part C: Emerging Technologies* 15 (2), 96-112.
- 497 (20) Kesting, A., Treiber, M., Helbing, D., 2007. “General Lane-Changing Model MOBIL for Car-
498 Following Models”. *Transportation Research Record: Journal of the Transportation Research*
499 *Board*, 1999, 86-94.
- 500 (21) van Winsum, W., de Waard, D., Brookhuis, K. A., 1999. Lane change maneuvers and safety
501 margins. *Transportation Research Part F: Traffic Psychology and Behavior* 2 (3), 139–149.
- 502 (22) Zheng, L., Ismail, K., Meng, X., 2014. “Freeway Safety Estimation using Extreme Value
503 Theory Approaches: a comparative study”. *Accident Analysis & Prevention*, 62, 32–41.
- 504 (23) Chovan, J., Tijerina, L., Alexander, G., Hendricks, D., 1994. *Examination of Lane Change Crashes*
505 *and Potential IVHS Countermeasures*. Technical Report. US DOT, NHTSA, Washington D.C.,
506 USA.
- 507 (24) Hidas, P., 2005. “Modelling vehicle interactions in microscopic simulation of merging and
508 weaving”. *Transportation Research Part C: Emerging Technologies* 13 (1), 37–62.
- 509 (25) Ben-Akiva, M. E., 1973. *Structure of passenger travel demand models*. Ph.D. thesis, Massachusetts
510 Institute of Technology, Cambridge, USA.
- 511 (26) Ben-Akiva, M. E., Lerman, S. R., 1985. *Discrete choice analysis: theory and application to travel*
512 *demand*. MIT Press, Cambridge, USA.
- 513 (27) Oh, C., Oh, J.-S., Ritchie, S., Chang, M., Jan. 2001. “Real-time estimation of freeway accident
514 likelihood”. In: *Proceedings of the 80th Annual Meeting of the Transportation Research Board*.
515 *Transportation Research Board*, Washington D.C., USA.
- 516 (28) Abdel-Aty, M., Uddin, N., Pande, A., 2005. “Split Models for Predicting Multivehicle Crashes
517 During High-Speed and Low-Speed Operating Conditions on Freeways”. *Transportation Research*
518 *Record: Journal of the Transportation Research Board* 1908, 51–58.
- 519 (29) Manski, C. F., Lerman, S. R., 1977. “The Estimation of Choice Probabilities from Choice Based

- 520 Samples". *Econometrica* 45 (8), 1977–88.
- 521 (30) Lima Azevedo, C. 2014, *Probabilistic safety analysis using traffic microscopic simulation*. PhD
522 Thesis, Instituto Superior Técnico, University of Lisbon, Portugal.
- 523 (31) Lima Azevedo, C., Cardoso, J. L. and Ben-Akiva, M. E., 2014a. "Applying Graph Theory to
524 Automatic Vehicle Tracking by Remote Sensing". *Proceedings of the 93rd Annual Meeting of the*
525 *Transportation Research Board*, Washington D.C., USA.
- 526 (32) Qi, Y., Koutsopoulos, H. N. and Ben-Akiva, M. E., 2000. "Simulation Laboratory for Evaluating
527 Dynamic Traffic Management Systems". *Transportation Research Record: Journal of the*
528 *Transportation Research Board*, 1710, 122-130.
- 529 (33) Ciuffo, B. and Lima Azevedo, C., 2014. "A Sensitivity-Analysis-Based Approach for the Calibration
530 of Traffic Simulation Models" *IEEE Transactions on Intelligent Transportation Systems* PP (99),
531 pp.1-12.
- 532 (34) Lima Azevedo, C., Ciuffo, B., Cardoso, J. L. and Ben-Akiva, M. E., 2014b. "Dealing with
533 uncertainty in detailed calibration of traffic simulation models for safety assessment". *Submitted to*
534 *Transportation Research Part C*.
- 535 (35) Inoue, T., Hioki, Y., 1993. "Skid resistance monitoring in Japan". *Roads* 280.
- 536 (36) Bierlaire, M., 2003. "BIOGEME: A free package for the estimation of discrete choice models". In:
537 *Proceedings of the 3rd Swiss Transportation Research Conference*. Ascona, Switzerland.
- 538 (37) Xu, C., Tarko, A. P., Wang, W., Liu, P., 2013. Predicting crash likelihood and severity on freeways
539 with real-time loop detector data. *Accident; Analysis & Prevention* 57, 30–9.